Proceedings World Geothermal Congress 2020+1
Reykjavik, Iceland, April - October 2021

Numerical Simulation of Fluid Flow and Heat Transfer in Hot Rocks with Single Fracture Considering THM Coupling Processes

Xu Zhang[a], Yang Li[a,b*], Jun Yao[a], Zhaoqin Huang[a] and Zhixue Sun[a]

[a] Research Centre of Multiphase Flow in Porous Media, China University of Petroleum (East China), Qingdao, China, 266580

[b] Department of Oilfield Exploration & Development, Sinopec, Beijing, China, 100728

xu.zhangupc@gmail.com, liyang@sinopec.com.cn

Keywords: Enhanced geothermal system; fractured rocks; THM coupling; aperture heterogeneity

ABSTRACT

The geothermal heat production from Enhanced Geothermal System (EGS) is influenced by complex thermal-hydraulic-mechanical (THM) coupling process, it is necessary to consider THM coupling effects on utilization efficiency and production performance of EGS. Based on local thermal non-equilibrium theory, a mathematical model incorporating THM coupling processes is established and rough fracture surface is generated based on fractal theory, to investigate the heat extraction performance in EGS with the consideration of fracture heterogeneity. An ideal three dimensional geothermal doublet numerical model is constructed to study the effects of thermal stress and nonhomogeneous aperture distribution on fluid flow pattern and heat transfer. The influence of match relationship between well pattern and fracture aperture distribution field on heat performance is evaluated through two index, average outlet temperature and thermal recovery. The results indicate that under the effects of aperture heterogeneity and thermal stress, the flow channeling phenomenon and early thermal breakthrough is occurred which makes the heat extraction response worse. As for aperture heterogeneity existed in fractured rocks, the injection and production wells should be arranged in vertical direction of high permeability zone to maintain longer heat mining time and improve thermal recovery.

1. INTRODUCTION

The fluid flow and heat transfer in hot fractured rock are the dominant processes of heat exploitation from enhanced geothermal system (EGS). The stimulation and management of EGS involves complex multi-physical processes, including thermal-hydrological-mechanical (THM) processes, and multi-scale effects. Therefore, it is of great significance to study the THM coupling processes in fractured porous media to reveal the mechanism of EGS thermal mining, predict its operating state, utilization efficiency, service life and handle the practical problems encountered in its development. Another Key issues existed in heat production from hot dry rock is flow channeling, which refers to concentration of fluid flow in a relatively small permeable region. Flow channeling will decrease contact area between cold fluid and hot rock, make production temperature drop quickly and worsen heat production performance.

In recent years, many useful models have been developed for modeling the performance of EGS. Chen et al. (2014) studied the heat exchange phenomena on fracture surface and proposed a coupled mathematical model to describe seepage and heat transfer based on discrete fracture network. Based on a three-dimensional transient model, Jiang et al. (2014) investigated the heat flow process of EGS reservoir by treating the heat reservoir as an equivalent porous medium. Xu et al. (2015) presented a simplified method to simulate the coupled thermal-hydraulic problem of heat mining in complex fractured rock mass, and verified the method in field application. Lei (2015) and Rutqvist et al. (2011) conducted secondary development based on TOUGH2 software, established the corresponding THM coupling model and solution method to realize the numerical simulation of EGS mining process. Bahrami (2015) simulated the THM coupling processes within a single fracture and studied the response characteristics of EGS based on the pore elasticity theory. Zhao et al. (2002, 2015) established a 3D THM coupling model of fractured media to simulate the extraction of HDR geothermal energy, by which the fracture area was discretely modeled by the Goodman joint element. Yao (2018) and sun et al. (2017) studied the characteristics of fluid flow, heat transfer and rock deformation of enhanced geothermal system under the consideration of THM coupling effects based on two-dimensional and three-dimensional discrete fracture network models. The above research results show that THM coupling processes will seriously affect the thermal production performance and must be taken into consideration to conduct EGS production simulation. However, the influence of fracture aperture heterogeneity on flow channeling is neglected, which still cannot truly reflect the actual formation situation.

In this work, a three-dimensional numerical model considering THM coupling effect was established to investigate fluid flow and heat transfer in low-permeability fractured crystalline rock. A single rough fracture was generated based on fractal theory to study its influence on thermal recovery performance of EGS. The effect of fracture aperture heterogeneity and thermal stress on flow pattern and heat production was analyzed through a 3D doublet well model with a single rough fracture. The influence of the matching relationship between well layout and fracture aperture field on thermal energy extraction was discussed with regard to two characteristic indexes, average production temperature and reservoir heat recovery. The simulation results of this study offer good insight to reveal physical mechanisms governing the flow channeling processes and offer good guidance for the design and optimization of EGS.

2. MODEL DESCRIPTION

2.1 Governing equations

The thermo-poroelastic model for fractured porous media has been constructed by Yao (2018) and sun et al. (2017). The geothermal reservoir is regarded as a fractured porous media consisting of rock matrix blocks and discrete fractures. Considering local thermal non-equilibrium between solid matrix and fluid, the model employs two energy conservation equations to describe heat transfer in

the matrix and the fractures respectively, which can reveal the actual subsurface heat exchange process during the development period. The effects of hydraulic loading and thermal stress are taken into account of the solid deformation.

The governing equations of THM coupling model in fractured porous media can be expressed as:

(1) Equilibrium equation

$$\sigma_{ij,j} + F_i = 0 \tag{1}$$

$$\frac{E}{2(1+\nu)} u_{i,jj} + \frac{E}{2(1+\nu)(1-2\nu)} u_{j,ji} - \alpha_B p_{,i} - \alpha_T \frac{E}{(1-2\nu)} T_{s,i} + F_i = 0 \tag{2}$$

Where, σ_{ij} is stress tensor, Pa; u represents displcement, m; F_i is body force, Pa; E and ν represent elastic modulus and poisson ratio respectively, Pa; p is pressure, Pa; α_B denotes Biot's coefficient, ≤ 1; T_s means matrix temperature, K; α_T is the coefficient of volumetric expansion corresponding to the bulk medium, 1/K; $\alpha_B p_{,i}$, $\alpha_T \frac{E}{(1-2\nu)} T_{s,i}$ represents hydraulic stress term and thermal stress term.

(2) Fracture deformation equation

$$u_n = \sigma_n' / k_n, \quad u_{s1} = \sigma_{s1}' / k_s, \quad u_{s2} = \sigma_{s2}' / k_s \tag{3}$$

$$\sigma_n' = \sigma_n - \alpha_B p, \quad \sigma_{s1}' = \sigma_{s1}, \quad \sigma_{s2}' = \sigma_{s2} \tag{4}$$

Where, k denotes fracture stiffness, Pa/m; u is displacement, m; σ' is effective stress, Pa; The subscripts "n" and "s" represent normal and tangential directions to the fracture plane respectively.

(3) Mass conservation equation in matrix

$$S \frac{\partial p}{\partial t} + \nabla \cdot u = -\frac{\partial e}{\partial t} + Q \tag{5}$$

$$u = -\frac{\kappa}{\eta}(\nabla p + \rho g \nabla z) \tag{6}$$

Where, t is time, s; u is flow velocity, m/s; κ is the intrinsic permeability of porous media, m^2; η is fluid dynamic viscosity, Pa·s; S is specific storage, 1/Pa; e is volumetric strain; Q represents fluid exchange on interface between rock matrix and fracture, 1/s。

(4) Mass conservation equation in fracture

$$d_f S_f \frac{\partial p}{\partial t} + \nabla_\tau \cdot (-d_f \frac{\kappa_f}{\eta} \nabla p) = -d_f \frac{\partial e_f}{\partial t} + Q_f \tag{7}$$

Where, S_f is the specific storage of fracture, 1/Pa; d_f denotes fracture aperture, m; κ_f is fracture permeability, obeys cubic law, $\kappa_f = \frac{d_f^2}{12f}$, m^2; f is fracture roughness; Q_f is the fluid exchange on the fracture surface between rock matrix and fracture, $Q_f = -\frac{\kappa_f}{\eta} \frac{\partial p}{\partial n}$, n represents the normal direction on the fracture surface; e_f is the volumetric strain of fracture; ∇_τ denotes the gradient operator restricted to the fracture's tangential plane.

(5) Energy conservation equation in matrix

$$(\rho C)_{eff} \frac{\partial T_s}{\partial t} = \lambda_{eff} \nabla^2 T_s + W \tag{8}$$

Where, $(\rho C)_{eff} = (1-\varepsilon)\rho_s C_s + \varepsilon\rho_f C_f$, $\lambda_{eff} = (1-\varepsilon)\lambda_s + \varepsilon\lambda_f$, ρ_s is matrix density, kg/m^3; λ_s denotes heat conductivity of matrix, W/m/K; C_s is matrix heat capacity, J/kg/K; W means heat exchange on the fracture surface between rock matrix and fracture, W/m^3.

Compared with the flow in fracture, water transport velocity in porous rock matrix is much smaller. Therefore, it can be assumed that the temperature of porous water is identical to that of rock. The heat advection in the pores has thus been overlooked.

(6) Energy conservation equation in fracture

$$d_f \rho_f C_f \frac{\partial T_f}{\partial t} + d_f \rho_f C_f \cdot u_f \nabla_\tau T_f = d_f \nabla_\tau \cdot \left(\lambda_f \nabla_\tau T_f\right) + W_f \tag{9}$$

Where, ρ_f is fluid density, kg/m^3; C_f is specific heat of water, J/kg/K; λ_f heat conductivity of water, W/m/K; u_f is fluid flow velocity in fracture, m/s; T_f is the water temperature in fracture, K; W_f means heat exchange on the fracture surface between rock matrix and fracture, W/m^2.

Assume that the heat exchange between rock matrix and fracture water follows the Newton's heat transfer law, the heat flow from the rock to the fracture water per unit area is defined as

$$W_f = h(T_s - T_f) \tag{10}$$

Where, h is heat convection coefficient, W/m^2/K.

(7) Energy conservation equation in surrounding formation

In the absence of groundwater flow, the heat transfer in surrounding formation is dominated through conduction and the energy conservation equation in soil mass is formulated as

$$C_s \rho_s \frac{\partial T_s}{\partial t} = \lambda_s \nabla^2 T_s + W \tag{11}$$

2.2 HM coupling effect

Hydraulic fracturing is an important methods of reservoir stimulation (Hofmann et al., 2014), and the stimulating fractures are the main flow channels to carry heat transmission fluid. The mechanical behavior occurred during EGS heat mining process will cause severe deformation of fracture structure in rock mass. Therefore, the aperture of the fractures, one of the most important parameter controlling the feasibility and the viability of EGS, will change as it is stress or strain dependent. Particularly, in the rock mass containing dense fracture networks, the more deformable fractures will be the primary flow pathways for the work fluid. Thus, stress variation can bring a considerable change to the fracture aperture. The understanding of the evolution law of the fracture aperture is an important aspect to study the hydraulic-mechanical (HM) coupling effect in fractured rock mass. The classic Barton-Bandis model (Bandis et al., 1983; Barton et al., 1985) is taken to describe the relationship between fracture aperture and effective normal stress:

$$A = A_{\max} - \frac{a\sigma_n^{'}}{1 + b\sigma_n^{'}} \tag{12}$$

Where, A is the aperture under effective normal stress, $\sigma_n^{'}$, m; A_{max} is the aperture at zero or minimum effective stress state. *a, b* are two material and state-specific parameters. Assuming that the aperture diminishes to zero as the effective stress approaches infinity so that the relationship between A_{max}, *a, b* is $A_{max}=a/b$.

2.3 TH coupling effect

The property of the work fluid is another important factor influencing the coupling effects. Under high pressure and high temperature conditions in the deep underground reservoir, the density of water, ρ_f is no longer a constant value, this can be expressed as a function of pressure and temperature (Zhao et al., 2015),

$$1/\rho_f = 3.086 - 0.899017 \times (647.25 - T)^{0.147166} - 0.39 \times (658.15 - T)^{-1.6}(p - 225.5) + \delta \tag{13}$$

Where T is water temperature, ^{o}C; p is absolute water pressure, Pa; δ is a function of "p" and "T", The value of δ does not exceed 6% of $1/\rho_f$, m^3/kg. The temperature of water also affects its dynamic viscosity, $\eta = \upsilon\rho_f$ in which υ is the kinematic viscosity of water. A commonly used empirical formula for the kinematic viscosity is (Hofmann et al., 2014)

$$\upsilon = \frac{0.01775}{1 + 0.033T_f + 0.000221T_f^2} \tag{14}$$

Therefore, the density and viscosity of water are directly related with the temperature, which can dramatically change the coupling process of water transport and heat transfer in the reservoir.

3. MODEL SETUP

3.1 Computational model

A large number of open connected fracture zones are the main characteristics of EGS hot reservoir which must be taken into consideration to conduct numerical experiment.

In general, rock mass with dense small fractures is usually treated as an equivalent porous media simplified through mature continuum theory, while large faults or major penetrating fractures are modeled as discrete fractures (Auradou et al., 2006). In practice, most of the heat-carrying fluid in EGS may migrate directly from the injection well to the production well through solely one or several major flow channels (Chen et al., 2013). Therefore, heat production from a horizontal penetrating rough fracture in a large body of low permeability hot crystalline rock was simulated. The model contains injection and production wells, one stimulated fracture connecting these two wells, equivalent porous media and surrounding formation. The stimulated reservoir was located at subsurface 1150 m and its size is 500 m ×500 m ×500 m. The radius of injection and production wellbore is set as 1.0 m with their separation distance 300 m and depth 1075 m. The size of surrounding formation determined as 1000 m ×1000 m ×1000 m. The system geometry is shown as Figure 1. The finite element software, COMSOL Multiphysics, is employed to conduct numerical implementation and the finite element model used in the study is depicted as Figure 2.

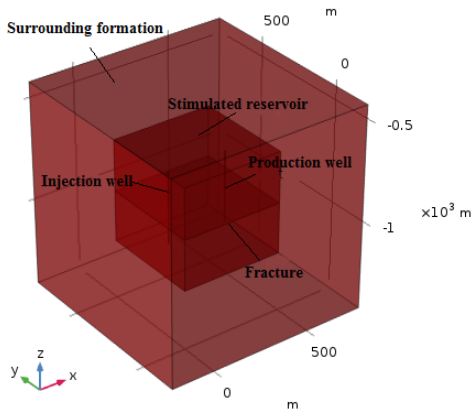

Figure 1 An ideal doublet well EGS model with single fracture

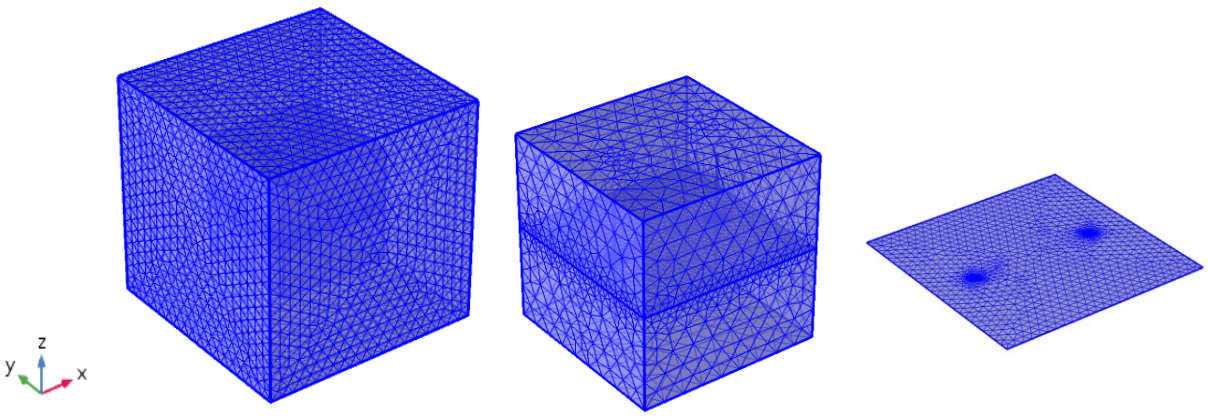

(a) Overall domain grids (b) Stimulated reservoir grids (c) Fracture surface grids

Figure 2 EGS finite element model with grid number 456876

3.2 Fractal rough fracture

A rough rock fracture surface is simulated according to fractal interpolation principle (Xie et al., 2001). Fractal fracture surfaces with different fractal dimensions and rough level can be generated by using a set of known fracture aperture value and different vertical scaling factors. As a larger vertical scaling factor is selected, a rougher fracture surface can be determined. A 3D fractal fracture surface is generated with regard to fractal theory, as shown in Figure 3, and heterogeneous aperture fields is obtained from the rough surface, depicted as Figure 4. Once the rough fracture is created, the statistical information of fracture aperture fields is gained. The

average fracture aperture is 0.178 mm with maximum fracture aperture 0.48 mm and minimum fracture aperture 3.07×10^{-6} mm, and the mean square deviation is 0.093 mm.

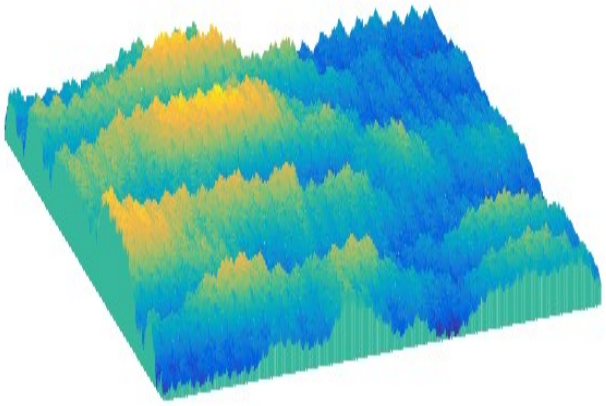

Figure 3 A sketch of 3D fractal fracture surface

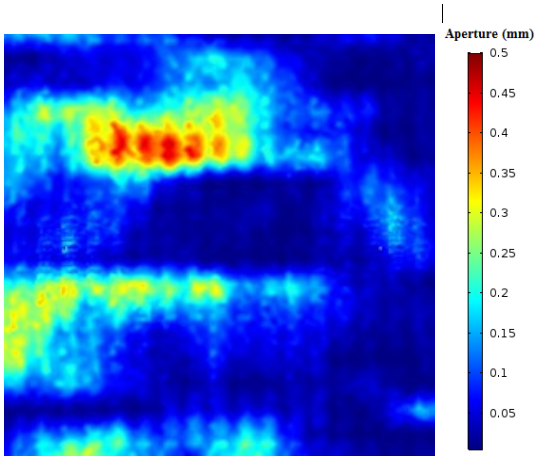

Figure 4 Heterogeneous fracture aperture field

The fracture aperture evolved with variable effective stress is determined by two constitutive parameters, a and b. In order to obtain the two material parameters, we can identify two reference states with effective normal stress, $\sigma'_{n,r1}$ and $\sigma'_{n,r2}$, and the corresponding fracture aperture field, A_{r1} and A_{r2}. According to formula 12, the two material and state-specific parameters can be calculated as

$$a = \frac{A_{r1}A_{r2}(A_{r2}-A_{r1})(\sigma_{r1}-\sigma_{r2})}{(\sigma_{r1}A_{r1}-\sigma_{r2}A_{r2})^2} \tag{15}$$

$$b = \frac{A_{r2}-A_{r1}}{\sigma_{r1}A_{r1}-\sigma_{r2}A_{r2}} \tag{16}$$

Then the independent variables are converted from a and b to Ar1 and Ar2, each simulation requires two aperture fields corresponding to two given reference stress states to fully quantify the deformation characteristics of the fracture. The initial natural state (effective normal stress 30MPa) is selected as the first reference state and above heterogeneous aperture field generated through fractal theory is treated as the fractured aperture corresponding to this stress state. The effective stress 5MPa was selected as the second reference stress state, and the fracture aperture under this state was assumed to be three times of that in the first reference state. The selected corresponding fracture apertures under the two stress states seems randomly due to the lack of realistic data to support a more practical model. However, it can fully reflect the most important deformable characteristics of rock fractures: fracture aperture and permeability will increase significantly with the decrease of effective stress (Guo et al., 2016).

Taking the average fracture aperture 0.178 mm under effective stress state 35 MPa and the the fracture aperture 0.534 mm under 5 MPa as an example, model parameters, a and b, are 1.186×10^{-10} 1/Pa and 1.333×10^{-7} 1/Pa, respectively. The corresponding A_{max} is 8.89×10^{-4} m. Therefore, the fracture aperture changed with effective stress can be calculated as

$$d_f = 8.89\times10^{-4} - \frac{1.186\times10^{-10}\sigma'_n}{1+1.333\times10^{-7}\sigma'_n} \tag{17}$$

3.3 Model parameters and conditions

(1) Model parameters

The reliability of numerical simulation results depends on the determination of computational parameters. However, relevant experimental and field application data are lacked in reality, the calculation parameters are chosen referred to previous numerical simulation cases as follows: water heat capacity 4200 J/kg/K, water thermal conductivity 0 W/m/K, matrix density 2700 kg/m^3, specific storage coefficient 1.0×10^{-9} 1/Pa, matrix permeability 1.0×10^{-20} m^2, elastic modulus 30 GPa, poisson's ratio 0.25, rock heat capacity 1000 J/kg/K, rock thermal conductivity 3 W/m/K, thermal expansion coefficient 3.0×10^{-6} K^{-1}, and porosity 0.01. The normal fracture stiffness is 800GPa/m, tangential stiffness is 400GPa/m. The acceleration of gravity is 9.8 m/s^2, Biot coefficient set as 1.0 and heat transfer coefficient is 3000 W/m^2/K.

(2) Initial and boundary conditions

As for stress field, the vertical stress is set as 64MPa, the minimum horizontal principal stress and maximum principal stress are 70MPa and 100MPa, respectively. This study applies the boundary condition of zero normal displacement on one boundary face in each direction and applies the specified in situ stress on the opposite boundary face in the same direction, which is a typical way of

applying in situ stress while eliminating the rigid body motion of the simulation system. The given pressure boundary conditions are used to ensure water circulating in the system. The left boundary is assumed to be the injection well with a given pressure of 55 MPa, and the right one is the production well at 34 MPa. For the other external conditions an impermeable boundary is selected. The initial water pressure in the reservoir is assumed as 34 MPa before water is injected. The temperature at the injection well is 60 °C. The top and bottom boundaries are thermal insulated. The initial temperature in the reservoir is 200 °C for both rock and water.

3.4 Characteristic parameters

1) Outlet production temperature

$$T_{out} = \frac{\int_L u_f d_f T_f dL + \iint_\Gamma u T_s d\Gamma}{\int_L u_f d_f dL + \iint_\Gamma u d\Gamma} \tag{18}$$

Where, the line integration term represents the fractures while the surface integration term represents the rock matrix blocks.

2) Overall heat recovery

For the purpose of explaining the local heat exchange in the reservoir and seeking for some methods to improve heat extraction performance, the local heat extraction ratio γ_L is employed and defined as the extracted heat divided by the stored or maximum extractable heat, which can be expressed as (Jiang et al., 2014)

$$\gamma_L(t) = \frac{T_r - T_s(t)}{T_r - T_{inj}} \tag{19}$$

Where, T_r and $T_s(t)$ is the initial rock temperature and the rock temperature at time instant t, respectively.

Furthermore, the overall heat recovery is obtained by the volume integral of local heat extraction ratio, which represents the ratio of the cumulative produced heat energy to the extractable heat energy. Simple derivation leads to the following equation

$$\gamma(t) = \frac{\iiint_V \gamma_L(t) dV}{\iiint_V dV} \tag{20}$$

4. RESULTS AND DISCUSSIONS

4.1 Analysis of thermal-hydraulic-mechanical processes

The temperature distribution in the reservoir, transverse and longitudinal cut view after 30 years production is presented in Figure 5. It can be seen that the temperature around fracture decreases rapidly due to convective heat transfer along the fracture surface. In addition, the flow pattern is unevenly distributed caused by heterogeneous fracture aperture field which leads to non-uniform heat exchange and makes part of hot regions undiscovered. As cooling front moves forward to the interface between fractured reservoir and impermeable surrounding rocks, heat is absorbed from the hot enclosing formation through the means of heat conduction which would slow down the reduction of heat storage temperature to some extent.

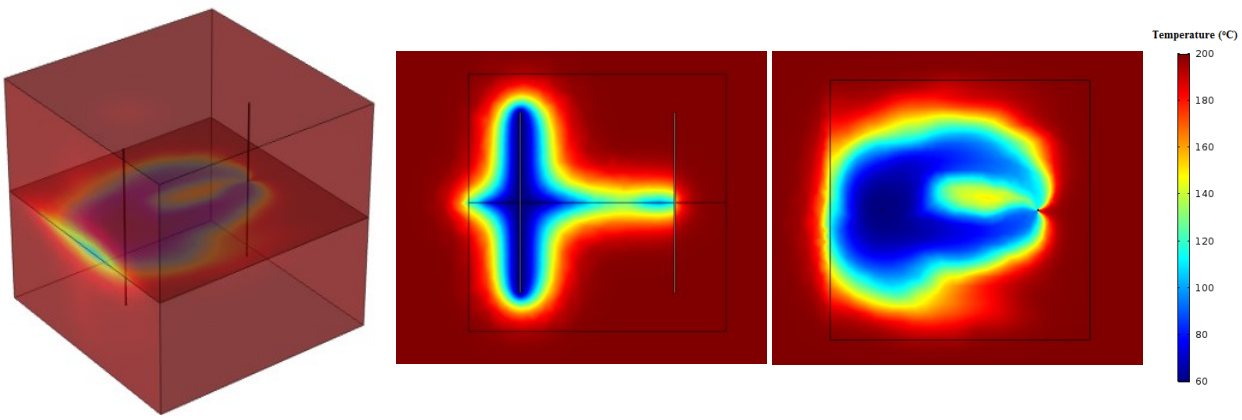

Figure 5 Temperature distribution in the stimulated reservoir, fracture surface and cut view at y = 250 m after 30 years.

Figure 6 demonstrates the evolutions of fracture permeability, flow velocity, temperature with and without considering thermal stress. Seen from the fracture permeability distribution, there are several high permeable regions and the injection and production wells are arranged along them. According to the fluid flow velocity field, we can find that concentration of heat transmission fluid occurs in the high permeable flow channels and forms short circulating flow paths. Then the reservoir temperature around short circulating flow paths drops rapidly and results in quick thermal breakthrough at production well. Hence, it is disadvantage to keep stable

production of EGS when heterogeneous fracture aperture inducing preferential flow paths existed and meanwhile, the injection and production wells are located along the direction of high permeable areas.

The evolution of fracture aperture along cutting line at y=250 m and x=150 m are displaced in Figure 7. With the progress of thermal mining, fracture aperture along the direction between injector and producer increases to a certain extent due to rock matrix cooling and contracting. As more cold fluid prefers to flow along the region with higher fracture aperture, it causes more heat extracted and temperature drops among these region and rock contracts more seriously, which will urge fracture opens to a greater extent. Compressive stress is prompted near the producing well by the reason of redistribution of stress and makes the fracture opening decrease.

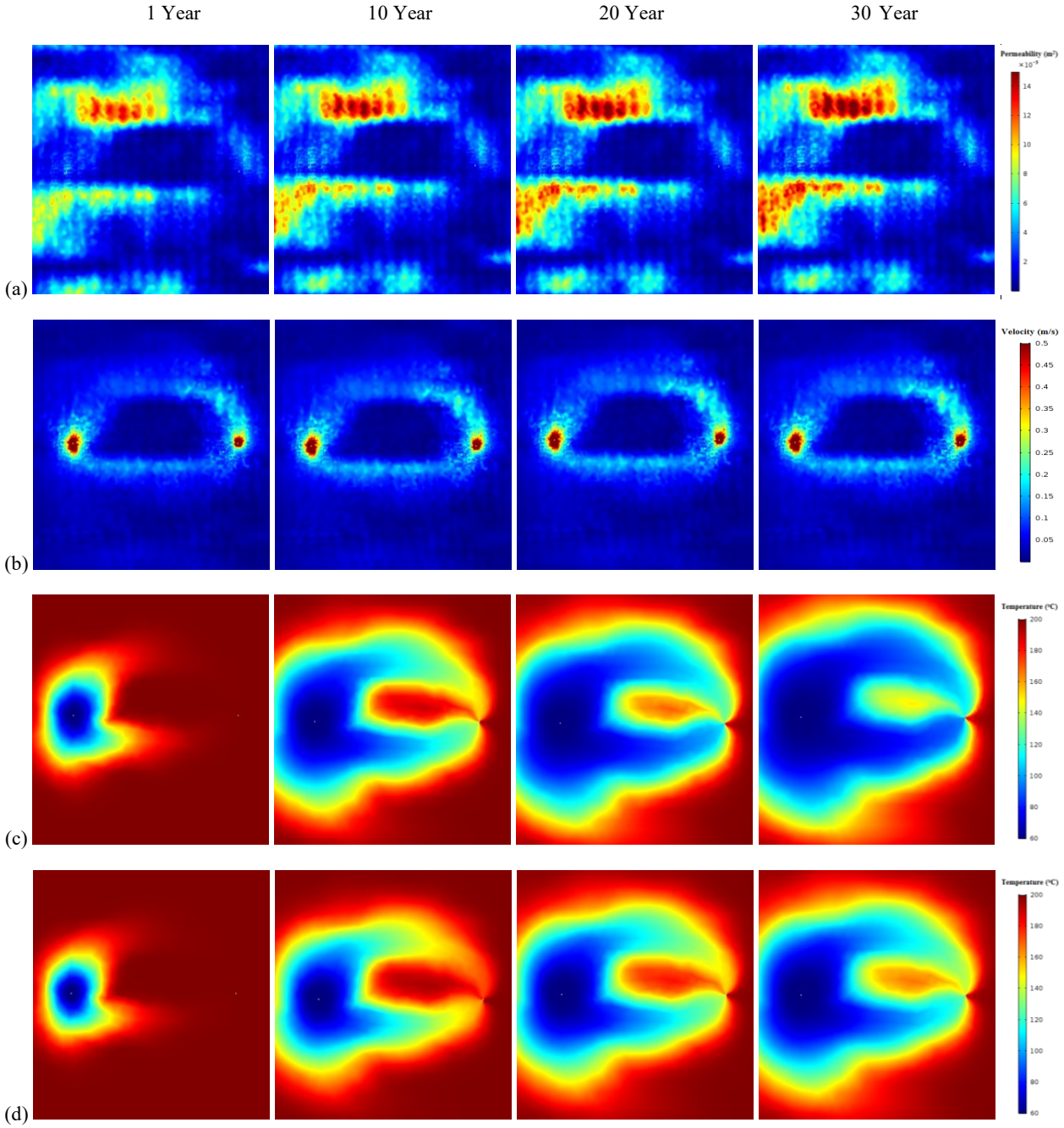

Figure 6 Evolution of (a) fracture permeability, (b) velocity, (c-d) temperature with and without considering thermal stress

In order to investigate the thermal effect on heat production performance, the comparison between considering and without considering thermal stress effect is made, as illustrated in Figure 6 (c) and (d). In the case of thermal mining under constant pressure drop, the region with temperature variation is broader in consideration of thermal stress acting on fractured porous media. The explanation of this phenomenon is that cold fluid injected into hot reservoir caused rock contracted and induced tensile thermal stress, which made fracture permeability grow up and fluid flow impedance reduce.

The changes of average outlet temperature and overall heat recovery over time with and without thermal stress are shown in Figure 8. When thermal stress effect is taken into account, the overall heat recovery after 30 years production is higher than that of without thermal stress impact, which conforms with the results of Figure 6 (c) and (d). However, the usage of geothermal energy mainly

depends on reservoir temperature, which can be directly utilized and generate electricity. Low-temperature fluid for electricity generation will lead to low thermal conversion efficiency (6-12%) (Zarrouk et al., 2014), and poor economic benefit. In order to generate electricity, the outlet temperature should be maintained higher than 150 ºC, otherwise, the production needs to be ceased. According to Figure 8, the reservoir service life is about 35 years without considering thermal stress and overall heat recovery is 8.2%. As for the case considering thermal stress, the operation time is 17.1 years and overall heat recovery is relatively low about 5.1%. Therefore, the thermal stress is of great importance to evaluate EGS heat production performance and must be taken into numerical simulation, otherwise, the lifetime and overall heat recovery will be overestimated and induce great difference.

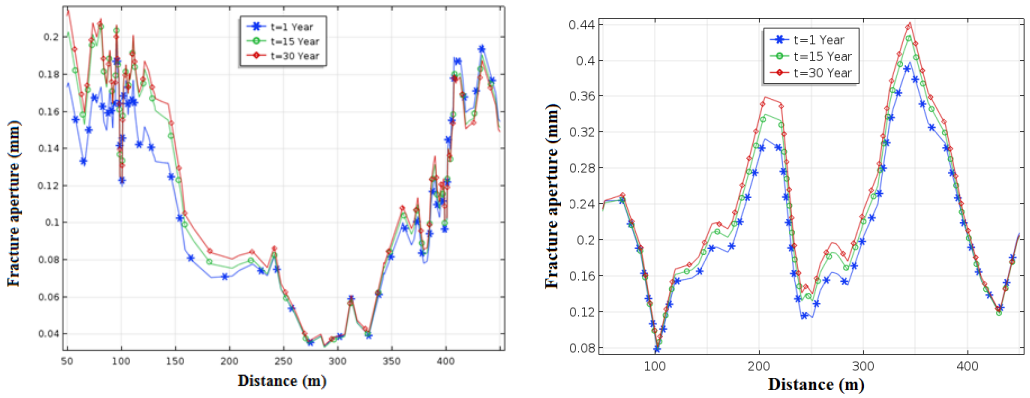

Figure 7 Evolution of fracture aperture along cutting line at y=250 m and x=150 m.

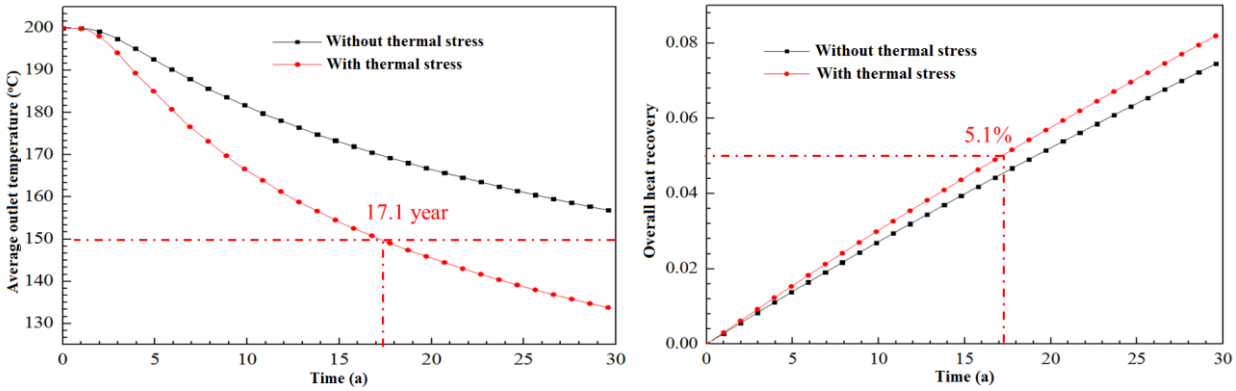

Figure 8 The changes of average outlet temperature and overall heat recovery over time with and without thermal stress

4.2 Effects of heterogeneity and thermal stress

Taken the average fracture aperture generated through fractal theory, in section 3.2, as the initial homogeneous fracture aperture, a thermal mining model of fractured rock mass with a homogeneous aperture fracture is established to study the influence of fracture heterogeneity and thermal stress on EGS production behavior. Evolution of fracture permeability, velocity, temperature with and without considering thermal stress under initial homogenous fracture aperture field is depicted in Figure 9. Compared with the case of heterogeneous aperture field, the flow pattern and temperature distribution in fracture are more uniform under homogeneous situation, which will prolong a stable exploitation lifetime. In view of thermal stress effect on homogeneous condition, the result is consistent with the heterogeneous one that the cold fluid sweep range is wider than that of without thermal stress.

Figure 10 illustrates evolution of the average outlet temperature over time with different combination of thermal stress and fracture aperture circumstance. It can be obtained that early thermal breakthrough is induced under the effects of thermal stress and heterogeneous fracture aperture. Meanwhile, the thermal stress causes heat production response worse in case of heterogeneous fracture aperture. Ultimately, the amount of heat production will be overestimated when fracture heterogeneity and thermal stress is neglected.

4.3 Effects of relationship between well layout and fracture aperture field

The aforementioned study investigated heat production response that injection-production wells located parallel to the high-permeability zone. In this section, the fracture aperture field of previous model is rotated by 90 degrees, as displaced in Figure 11, to make injector-producer perpendicular to the high-permeability zone for thermal recovery simulation.

The average outlet temperature and overall heat recovery varied with time under different wells-aperture field matching pattern is illustrated in Figure 12. The production lifetime and heat recovery are the lowest, in the case of parallel matching pattern, corresponding to 17.1 years and 5.1% respectively. A large amount heat remains in the hot fractured reservoir. As for homogeneous fracture aperture field, lifetime and recovery are moderate, corresponding to 26.8 years and 8.2%. For the presence of fracture aperture heterogeneity, reservoir lifespan and overall heat recovery are highest when injector-producer is perpendicular to large aperture zone,

about 50 years and 16%. In consequence, perpendicular matching pattern is preferred to achieve longer reservoir service lifespan and larger amount of extraction heat.

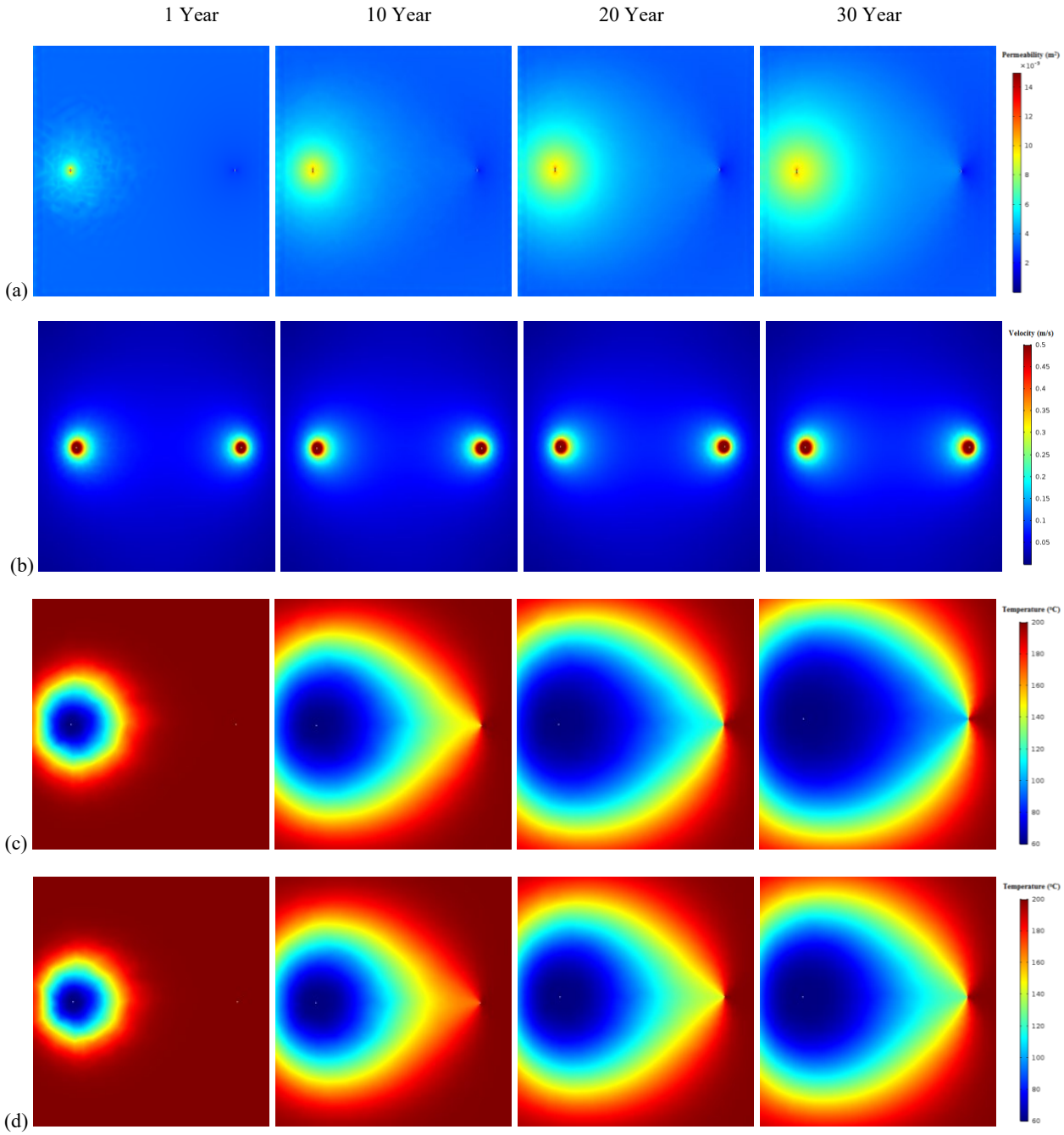

Figure 9 Evolution of (a) fracture permeability, (b) velocity, (c-d) temperature with and without considering thermal stress under initial homogenous fracture aperture field

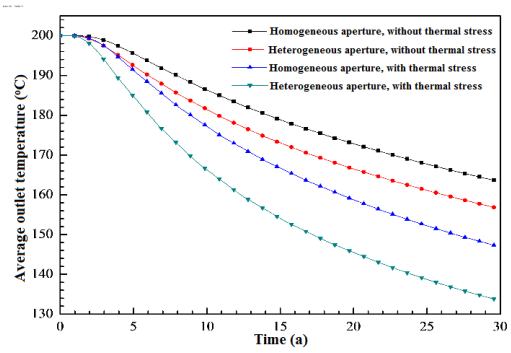

Figure 10 Evolution of the average outlet temperature with time.

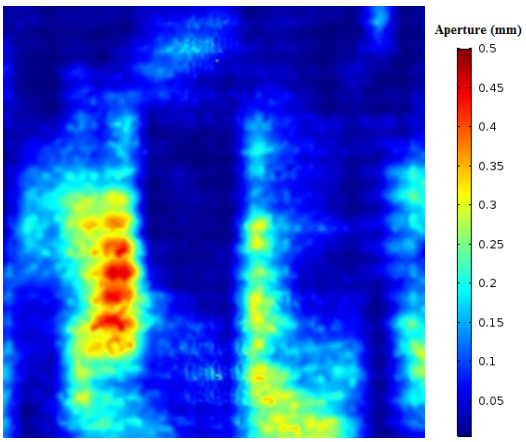

Figure 11 Rotated fracture aperture field

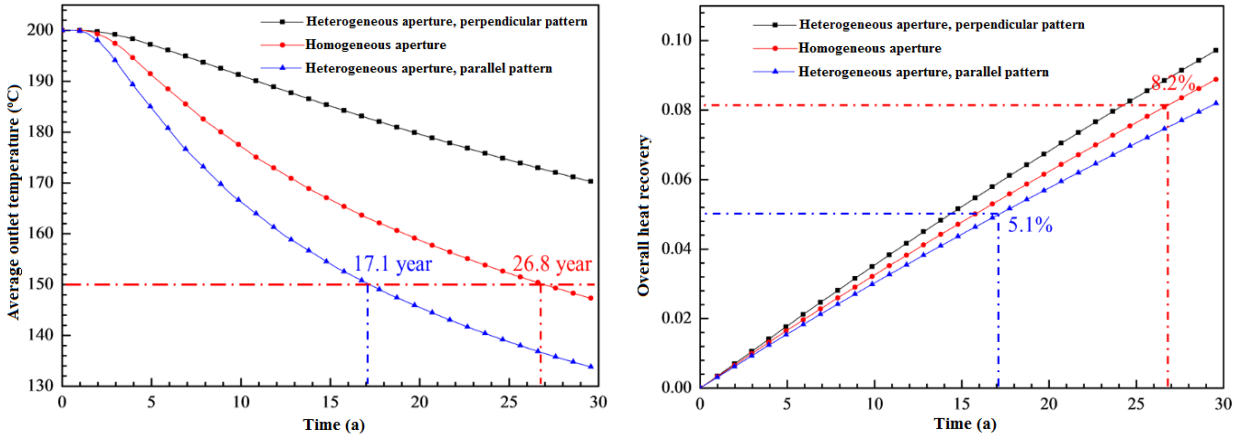

Figure 12 Average outlet temperature and overall heat recovery varied with time under different matching pattern

5. CONCLUSIONS

In this work, a three-dimensional numerical model considering THM coupling effect was established to investigate fluid flow and heat transfer in low-permeability fractured crystalline rock. A single rough fracture was generated based on fractal theory to study its influence on thermal recovery performance of EGS. The effect of fracture aperture heterogeneity and thermal stress on flow pattern and heat production was analyzed through a 3D doublet well model with a single rough fracture. The influence of the matching relationship between well layout and fracture aperture field on thermal energy extraction was discussed with regard to two characteristic indexes, average production temperature and reservoir heat recovery.

(1) A rough fracture surface is generate based on fractal theory to simulate THM response of EGS with heterogeneous fracture aperture field. Most fluid seepages along preferential channels due to the unevenly distributed fracture aperture. If injector-producer are located parallel to high permeable zones, thermal stress induced by cold fluid injected will further promote the formation of short cutting flow channels which makes the temperature around flow channels drop rapidly and early thermal breakthrough arise at production well.

(2) The heat production performance of hot fractured porous media considering THM coupling effects is investigated and the results show that the thermal stress has significant influence on fluid flow and heat transfer. Compared with the case of homogeneous fracture, its effect is more distinct in the view of fracture with heterogeneous aperture field which force the existence of flow channeling and worse heat mining response. For a better understanding of the performance of EGS, studies on the THM coupling in fractured rock mass are required.

(3) As for fractured rock mass with unevenly distributed fracture aperture, injection and production wells should be drilled perpendicular to the high permeable zones to reach longer reservoir service lifespan and higher heat recovery.

ACKNOWLEDGEMENT

This study was jointly supported by the National Natural Science Foundation of China (Grant No. 51774317) and the Graduate School Innovation Program of China University of Petroleum (Grant No. YCX2019015)

REFERENCE

Chen B, Song E, Cheng X H. A numerical method for discrete fracture network model for flow and heat transfer in two-dimensional fractured rocks[J]. Chinese Journal of Rock Mechanics and Engineering, 2014, 33(1): 43-51.

Jiang F, Chen J, Huang W, et al. A three-dimensional transient model for EGS subsurface thermo-hydraulic process. Energy, 2014, 72(7):300-310.

Xu C., Dowd P.A., Tian Z.F.. A simplified coupled hydro-thermal model for enhanced geothermal systems [J]. Applied Energy, 2015, 140: 135-145.

Lei H, Xu T, Jin G. TOUGH2Biot–A simulator for coupled thermal–hydrodynamic–mechanical processes in subsurface flow systems: Application to CO2 geological storage and geothermal development[J]. Computers & Geosciences, 2015, 77: 8-19.

Rutqvist J. Status of the TOUGH-FLAC simulator and recent applications related to coupled fluid flow and crustal deformations[J]. Computers & Geosciences, 2011, 37(6): 739-750.

Bahrami D, Danko G, Fu P, et al. Poroelastic and Self-Propped Single Fracture THM Models for EGS Studies[C]//proceedings of the 40th Stanford Geothermal Workshop, Stanford, California, USA. 2015.

Zhao Y, Wang R, Hu Y, et al. 3D numerical simulation for coupled THM of rock matrix-fractured media in heat extraction in HDR[J]. Chinese Journal of Rock Mechanics and Engineering, 2002, 21(12): 1751-1755.

Zhao Y, Feng Z, Feng Z, et al. THM (Thermo-hydro-mechanical) coupled mathematical model of fractured media and numerical simulation of a 3D enhanced geothermal system at 573 K and buried depth 6000–7000 M[J]. Energy, 2015, 82: 193-205.

Yao J, Zhang X, Sun Z, et al. Numerical simulation of the heat extraction in 3D-EGS with thermal-hydraulic-mechanical coupling method based on discrete fractures model[J]. Geothermics, 2018, 74: 19-34.

Sun Z, Zhang X, Xu Y, et al. Numerical simulation of the heat extraction in EGS with thermal-hydraulic-mechanical coupling method based on discrete fractures model[J]. Energy, 2017, 120: 20-33.

Hofmann H, Babadagli T, Zimmermann G. Hot water generation for oil sands processing from enhanced geothermal systems: Process simulation for different hydraulic fracturing scenarios[J]. Applied Energy, 2014, 113(1):524-547.

Bandis S C, Lumsden A C, Barton N R. Fundamentals of rock joint deformation[C]//International Journal of Rock Mechanics and Mining Sciences & Geomechanics Abstracts. Pergamon, 1983, 20(6): 249-268.

Barton N, Bandis S, Bakhtar K. Strength, deformation and conductivity coupling of rock joints[C]//International journal of rock mechanics and mining sciences & geomechanics abstracts. Pergamon, 1985, 22(3): 121-140.

Auradou H, Drazer G, Boschan A, et al. Flow channeling in a single fracture induced by shear displacement[J]. Geothermics, 2006, 35(5-6): 576-588.

Chen J, Jiang F, Luo L. Numerical simulation of down-hole seepage flow in enhanced geothermal system[J]. Chin. J. Comput. Phys, 2013, 30: 871-878.

Xie H, Sun H, Ju Y, et al. Study on generation of rock fracture surfaces by using fractal interpolation[J]. International Journal of Solids and Structures, 2001, 38(32-33): 5765-5787.

Guo B, Fu P, Hao Y, et al. Thermal drawdown-induced flow channeling in a single fracture in EGS[J]. Geothermics, 2016, 61: 46-62.

Zarrouk S J, Moon H. Efficiency of geothermal power plants: A worldwide review[J]. Geothermics, 2014, 51: 142-153.